NICOLAUS COPERNICUS UNIVERSITY IN TORUŃ

Bulletin of Geography. Physical Geography Series, No. 28 (2025): 81–101
http://doi.org/10.12775/bgeo-2025-0006

Gravity-anomaly-based analysis of surface ruptures along the Palu-Koro Fault (Indonesia) for long-term seismic hazard mitigation

Muhammad Frando[1][a], Puji Ariyanto[2][b], Joshua Purba[3][c]*, Thea Monica Apriliaji[1][d]

[1]Bandung Geophysical Station, Agency for Meteorology Climatology and Geophysics (BMKG), Bandung, Indonesia
[2]Indonesian State College of Meteorology, Climatology, and Geophysics (STMKG), Tangerang, Indonesia
[3]Gowa Geophysical Station, Agency for Meteorology Climatology and Geophysics (BMKG), Gowa, Indonesia

*E-mail: joshua.purba@bmkg.go.id

[a]https://orcid.org/0009-0004-5682-3986, [b]https://orcid.org/0000-0001-7309-5192, [c]https://orcid.org/0009-0006-7959-8288, [d]https://orcid.org/0009-0009-7250-4252

Abstract. The Palu-Koro Fault system in Central Sulawesi is a major strike-slip fault associated with significant seismic hazards. This study investigates the fault dynamics and associated surface ruptures using gravity anomaly data and derivative-based geophysical methods. The Simple Bouguer Anomaly (SBA) values, ranging from –2 to 56 mGal, reveal substantial density contrasts in the subsurface, delineating fault boundaries and localised geological structures. Residual anomaly maps highlight sharp density gradients, which correspond to active fault zones. The derivative analyses, including First Horizontal Derivative (FHD) and Second Vertical Derivative (SVD), further refine the fault geometry and movement mechanisms, confirming the predominantly strike-slip nature of the Palu-Koro Fault, with localised normal faulting in certain segments, particularly in pull-apart basins and fault stepovers. The identified fault structures are consistent with previously mapped surface ruptures and aftershock distributions, indicating a strong correlation between gravity-derived density contrasts and active fault segmentation. These findings offer critical insights into fault behaviour, contributing to more accurate seismic hazard assessments and disaster mitigation strategies. The results reinforce the importance of gravity-based geophysical techniques in fault characterisation and highlight their potential for integration with other geophysical datasets in seismic hazard analysis.

Key words:
Indonesia,
Palu City,
Surface Rupture,
Gravity Anomaly,
Derived Method

Introduction

The tectonic framework of the Palu region in Central Sulawesi, Indonesia, is characterised by a highly complex interaction of active fault systems, including the Palu-Koro Fault (Fig. 1a, b). This fault is one of the primary tectonic features responsible for the region's high seismicity (Bellier et al. 2001; Watkinson 2011; Fang et al. 2019). The convergence of major tectonic plates – the Pacific Plate, the Indo-Australian Plate, and the Eurasian Plate – has led to the formation of active faults with varying mechanisms, including strike-slip, reverse and normal faulting (Hall 2002; Irsyam et al. 2020; Yu and Sun 2022). The Palu-Koro Fault, extending ~500 km from the Makassar Strait to the Bone Bay, is a left-lateral strike-slip fault and represents a significant seismic hazard for the area (Walpersdorf et al. 1998; BMKG 2019; Supendi et al. 2019; BMKG 2023; Purba et al. 2024).

A significant tectonic earthquake that struck Palu occurred on September 28, 2018, with a magnitude of Mw 7.5, demonstrating the destructive potential of the Palu-Koro Fault. The Global Centroid Moment Tensor (GCMT) solution for this event (Fig. 1a) indicates a predominantly strike-slip faulting mechanism with minor oblique components. The first nodal plane (strike =

348°, dip = 57°, slip = –15°) closely aligns with the mapped geometry of the Palu-Koro Fault by PuSGeN (2017), confirming left-lateral motion along a north-northwest (NNW) striking plane. Meanwhile, the second nodal plane (strike = 87°, dip = 77°, slip = –146°) suggests an alternative fault plane with a steeper dip, likely accommodating secondary faulting (Ekström et al. 2014). Focal mechanism solutions provide critical insights into fault slip direction and orientation, serving as essential tools for characterising fault zones and regional stress regimes based on seismic data (Khalid et al. 2015; Cheng et al. 2023; Rong et al. 2023).

The 2018 Palu earthquake not only produced complex fault rupture patterns but also triggered cascading hazards, including tsunamis and extensive liquefaction, leading to widespread displacement and significant loss of life. By October 21, 2018, the disaster had claimed 2,256 lives, with fatalities distributed across the affected regions: 1,703 in Palu, 171 in Donggala, 366 in Sigi, 15 in Parigi Moutong, and 1 in Pasangkayu. In addition, 1,309 people were reported missing, 4,612 were injured, and 223,751 were displaced across 122 evacuation sites (Valkaniotis et al. 2018; BNPB 2019; Natawidjaja et al. 2021). Notably, the earthquake's surface rupture deviated from the fault line previously mapped by PuSGeN (2017), traversing densely populated areas in Palu (Ekström et al. 2014; Valkaniotis et al. 2018; Natawidjaja et al. 2021). This raises critical concerns for urban planning and disaster mitigation, emphasising the need for accurate mapping and proactive strategies to address such hazards in the future (Daryono 2016; Valkaniotis et al. 2018; Purba et al. 2024).

The difference between the observed surface rupture and the mapped trajectory of the Palu-Koro Fault (Fig. 1b) communicates a gap in understanding the fault's detailed behaviour and seismic hazards associated with such activity. Traditional seismic hazard models often rely upon historical fault mapping, which may not capture unmapped or secondary faults. This study therefore seeks to improve disaster mitigation strategies by using gravity anomaly data to delineate fault structures and surface ruptures in a more accurate manner (Stanley 1977; Reynolds 1997; Biasi and Wesnousky 2016; Valkaniotis et al. 2018; Burger et al. 2023).

Gravity anomaly analysis has been widely recognised as a powerful tool for investigating subsurface geological structures, particularly in seismically active regions. By analysing variations in Bouguer Anomaly values, geophysicists can infer density contrasts associated with fault zones, which are critical for understanding fault dynamics and identifying potential rupture zones (Blakely 1995; Hiramatsu et al. 2019; Eppelbaum et al. 2020; Umar 2023). Advanced techniques such as First Horizontal Derivative (FHD) and Second Vertical Derivative (SVD) further enhance this analysis by delineating the boundaries of geological structures with greater precision (Elkins 1951; Stanley 1977; Reynolds 1997; Fedi and Florio 2001; Du and Zhang 2021).

The Palu-Koro Fault system, as depicted in the geological map (Fig. 1b,c) provides a critical context for such analyses. The alignment of varying lithologies, including clastic sedimentary rocks, metamorphic sequences and alluvium, highlights the complex tectonic evolution of the area (Sukamto 1982; Natawidjaja et al. 2021). Integrating gravity anomaly analysis with these mapped geological features enables a more detailed delineation of fault zones and their associated density contrasts, particularly for the Palu-Koro Fault, where surface rupture and lithological variations suggest significant subsurface heterogeneity.

In the context of active fault mapping, these methods have been applied successfully in various tectonic settings. For example, FHD and SVD techniques can highlight regions with abrupt density contrasts, which often correspond to fault zones (Rosid and Siregar 2017; Dewanto et al. 2022; Rosid 2023; Murdapa et al. 2024). Such analyses provide critical insights into the movement mechanisms of strike-slip faults, including those similar to the Palu-Koro Fault, by identifying patterns of stress accumulation and release along fault lines. Integrating these gravity-based methods with other geophysical tools, such as seismic and remote sensing data, has proven effective in creating comprehensive fault models that improve hazard assessments (Fedi and Florio, 2001; Du and Zhang, 2021; Purba et al. 2024).

Although the Palu-Koro Fault is well-documented, gaps remain in understanding the interactions between major and secondary faults. Studies such as those by Bellier et al. (2001), Daryono (2016) and Valkaniotis et al. (2018)

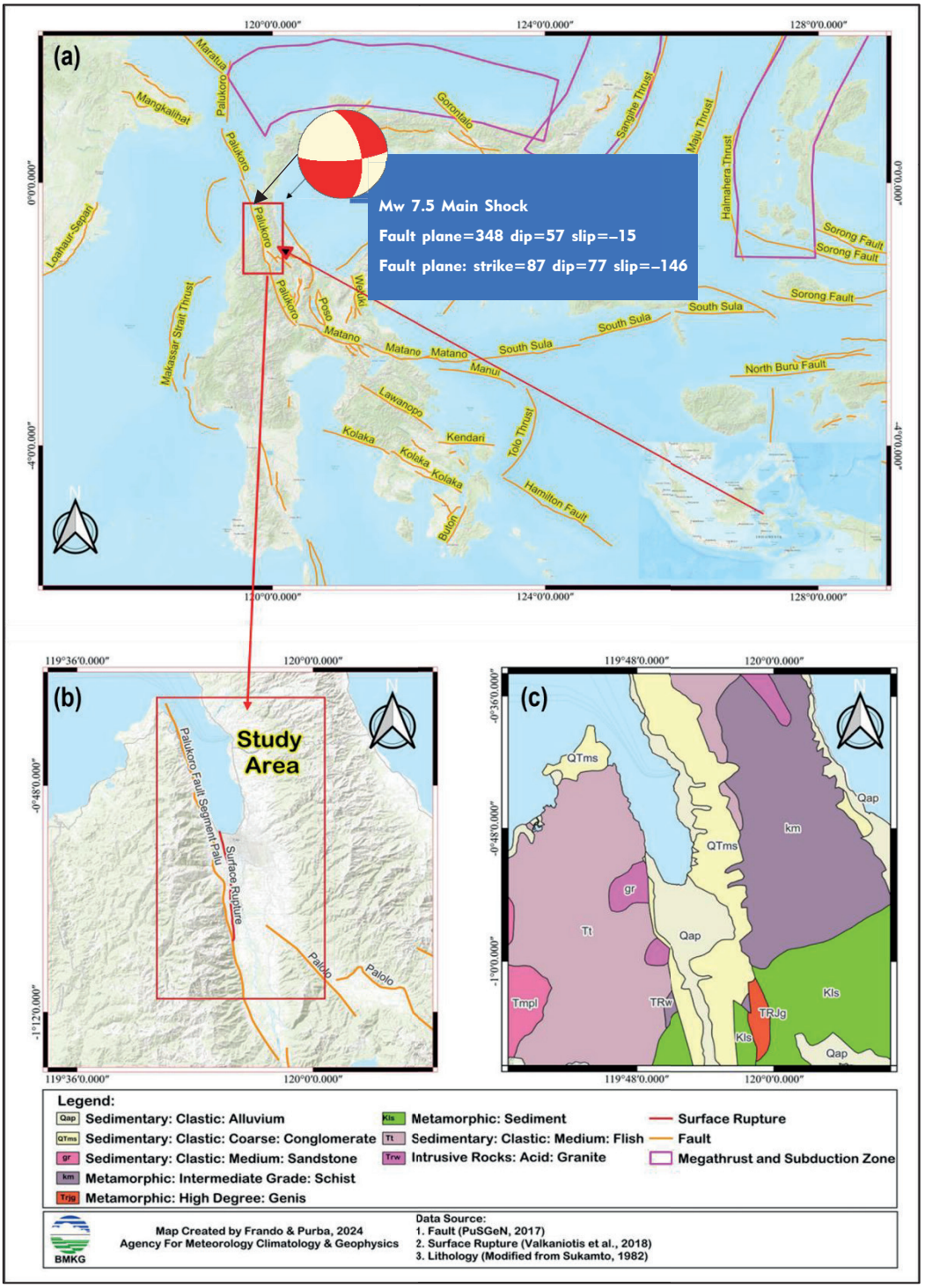

Fig. 1. Map of Tectonic and geological setting around Sulawesi and the study area: a) Distribution of active faults and centroid moment tensor (CMT) solution of the 2018 Mw 7.5 Palu earthquake (modified from Ekström et al. 2012; Irsyam et al. 2020; PuSGeN 2017, 2022, 2024); b) Location of the Palu-Koro Fault segment within the study area (modified from PuSGeN 2017); c) Geological formations surrounding the study area (modified from Sukamto 1982)

have identified the fault's significant role in the region's tectonics but do not fully account for the observed deviations in rupture patterns during the 2018 earthquake. Furthermore, traditional geological mapping techniques fail to capture the complexities of fault behaviour in urbanised settings (Daryono 2016; Andriamamonjisoa and Hubert-Ferrari 2019; Valkaniotis et al. 2018; Williams et al. 2020).

Advanced geophysical methods, such as gravity gradient analysis and satellite-based remote sensing, have shown promise in addressing these gaps. However, their application in the Palu region remains limited, particularly in integrating derivative analyses with geological data to enhance fault mapping and seismic risk assessment (Bellier et al. 2001; Daryono 2016; Purba et al. 2024). This lack of comprehensive data integration represents a critical research gap.

The primary objective of this study is to investigate the surface rupture patterns associated with the Palu-Koro Fault and their relationship to gravity anomalies. In addition, this study aims to provide a scientific foundation for long-term earthquake hazard mitigation in the Palu region by identifying active fault segments and understanding their subsurface characteristics. Specifically, the study seeks to determine the extent to which gravity-based analyses, such as FHD and SVD, can be used to accurately delineate fault structures and predict potential surface rupture zones.

The novelty of this research lies in its application of derivative-based gravity analysis techniques to the Palu-Koro Fault system, which has not been extensively explored in previous studies. By integrating these methods with existing geological and seismic data, the study aims to provide a more comprehensive model of fault dynamics and rupture behaviour. This innovative approach addresses the limitations of traditional mapping techniques and offers new insights into the complex interactions between primary and secondary fault systems.

The scope of the study includes the use of gravity anomaly data to identify and analyse the spatial characteristics of surface ruptures, with a particular focus on their implications for disaster mitigation and urban planning. The findings are expected to guide local government policies while providing a valuable reference for geophysical researchers studying Palu City and other regions. Ultimately, this research aims to enhance community resilience and preparedness (mitigation) against future seismic events.

Materials and methods

Gravity

Gravity is central to one of the geophysical methods based on the measurement of variations in the acceleration value of the earth's gravity (Telford et al. 1990; Gabo et al. 2015; Phillips 2015). This method is used to identify and describe the shape of subsurface geological structures based on variations in the Earth's gravity field produced by density differences between rocks (Telford et al. 1990; Phillips 2015). This method studies variations in gravity acceleration value due to variations in rock mass density in the subsurface. Therefore, this research focuses on the difference in the acceleration value of gravity from one observation point to another. One of the applications of the gravity method is to map geological structures in the form of faults (Sarkowi 2010; Layade et al. 2020; Khogali et al. 2024). Therefore, this method can be used to estimate locations and types of faults.

In this study, the author estimates the location of the fault in the study area based on the Simple Bouguer Anomaly response and the First Horizontal Derivative and Second Vertical Derivative analysis.

Simple Bouguer Anomaly

The Simple Bouguer Anomaly (SBA) is a widely used gravity anomaly in fault interpretation studies, representing the difference between the observed gravity value and the theoretical (normal) gravity value (Gabo et al. 2015; Armada et al. 2020; Layade et al. 2020). The SBA in this study was calculated without explicit terrain corrections, as the primary objective was to identify fault structures rather than to refine absolute gravity values. Although terrain effects can influence SBA computations, previous

studies (Sembiring et al. 2023; Godah et al. 2024) have shown that these effects are more pronounced in regions with significant topographic relief. Given that the Palu region exhibits moderate elevation variations, the omission of terrain correction is unlikely to introduce significant biases in the identification of fault-related anomalies.

Furthermore, SBA results derived from GGM-plus data already incorporate a degree of terrain modelling, reducing the need for additional correction steps (Pavlis et al. 2012). However, it is acknowledged that residual terrain effects may still be present, potentially contributing to localised variations in FHD and SVD results, particularly in areas with steep density contrasts (Gunawan and Permana 2024). The SBA value in this study was computed using the following equation (Blakely 1995):

$$\mathrm{SBA} = (g_{obs} - g_{\theta} + 0.3085h) - (0.04192\,\rho h) \quad (1)$$

$$\mathrm{SBA} = \mathrm{FAA} - \mathrm{BC} \quad (2)$$

Where SBA is the Simple Bouguer Anomaly, g_{obs} is the observed gravity, g_0 is normal/theoretical gravity at the relevant latitude, p is the mass density, h is the measurement altitude, FAA is the free air anomaly, and BC is the Bouguer correction.

First Horizontal Derivative (FHD)

First Horizontal Derivative (FHD) is a method used to show the boundary of a geological structure based on its weight anomaly seen from the change in the weight anomaly value from one point to another horizontally with a certain distance, which has sharp characteristics in the form of maximum or minimum values at the anomalous contact. This method is formulated as follows (Stanley 1977; Sarkowi et al. 2022):

$$\mathrm{FHD} = \sqrt{\left(\frac{\partial g}{\partial x}\right)^2 + \left(\frac{\partial g}{\partial y}\right)^2} \quad (3)$$

Where: $\frac{\partial g}{\partial x}$ and $\frac{\partial g}{\partial y}$ are the first derivative of the Earth's gravity field in the x and y directions, respectively.

Second Vertical Derivative (SVD)

The Second Vertical Derivative (SVD) is the second-order derivative value of the gravity anomaly, which is used to bring out the shallow effects of its regional influence and also to determine the boundaries of the structures present in the study area. Mathematically, the Second Vertical Derivative method can be obtained from the horizontal derivative because the gravity field satisfies the Laplace equation (Elkins 1951; Saibi et al. 2016; Sarkowi et al. 2022): (4)

$$\nabla^2 \Delta g = 0 \quad \text{with} \quad \nabla^2 \Delta \mathrm{g} = \frac{\partial^2(\Delta \mathrm{g})}{\partial \mathrm{x}^2} + \frac{\partial^2(\Delta \mathrm{g})}{\partial \mathrm{y}^2} + \frac{\partial^2(\Delta \mathrm{g})}{\partial \mathrm{z}^2}$$

So, the equation becomes:

$$\frac{\partial^2(\Delta \mathrm{g})}{\partial \mathrm{x}^2} + \frac{\partial^2(\Delta \mathrm{g})}{\partial \mathrm{y}^2} + \frac{\partial^2(\Delta \mathrm{g})}{\partial \mathrm{z}^2} = 0 \quad (5)$$

$$\frac{\partial^2(\Delta \mathrm{g})}{\partial \mathrm{z}^2} = -\left[\frac{\partial^2(\Delta \mathrm{g})}{\partial \mathrm{x}^2} + \frac{\partial^2(\Delta \mathrm{g})}{\partial \mathrm{y}^2}\right]$$

Since the value of y is constant for each incision or cross-section data, equation 5 becomes:

$$\frac{\partial^2(\Delta g)}{\partial z^2} = -\left(\frac{\partial^2(\Delta g)}{\partial x^2}\right) \quad (6)$$

The first derivative in the one-dimensional case can be found by dividing the difference of the gravity values at two locations (x(i) and x(i+1)) against the distance between the two locations *(Δx)*

$$\frac{\partial \Delta g(x_i)}{\partial x} = \frac{\{g(x_{i+1}) - g(x_i)\}}{\Delta x} \quad (7)$$

Then, the second derivative is calculated by finding the difference between the first derivatives of the two adjacent points, which results in the following equation:

$$\frac{\partial^2 \Delta g(x_i)}{\partial x^2} = \frac{\{g(x_3) - 2g(x_2) + g(x_1)\}}{(\Delta x)^2} \quad (8)$$

From the equations above, it can be seen that the Second Vertical Derivative of a surface gravity anomaly is the negative value of the derivative obtained through its horizontal second-order derivative. Meanwhile, the method used in this study to classify fault types is adapted from the approach introduced by Bott (1962),

which originally aimed to determine the slope direction of subsurface density boundaries, such as the interface between sedimentary basins and basement rocks. Bott (1962) demonstrated that the second vertical derivative (SVD) of a gravity anomaly highlights density contrasts, with the relative magnitudes of the maximum and minimum SVD values providing insight into the geometry of subsurface structures. In this study, this principle has been adapted to classify fault types by analysing the maximum and minimum values of the SVD, based on the assumption that variations in density gradients reflect different faulting mechanisms. While this adaptation provides a useful tool for fault delineation, it is important to acknowledge that SVD alone does not directly determine fault kinematics and should be interpreted alongside seismic (Supendi et al. 2019, 2020) and geological data (Sukamto 1982; Natawidjaja et al. 2021) for greater accuracy. To determine the type of fault structure can be determined by using the equation (Bott 1962; Sarkowi 2010; Reynolds 1997).

$$\left|\frac{\partial^2(\Delta g)}{\partial z^2}\right|_{min} > \frac{\partial^2(\Delta g)}{\partial z^2}_{max} \quad \text{=Reverse Fault}$$

$$\left|\frac{\partial^2(\Delta g)}{\partial z^2}\right|_{min} < \frac{\partial^2(\Delta g)}{\partial z^2}_{max} \quad \text{= Normal Fault}$$

$$\left|\frac{\partial^2(\Delta g)}{\partial z^2}\right|_{min} \approx \frac{\partial^2(\Delta g)}{\partial z^2}_{max} \quad \text{= Strike slip fault}$$

This research utilises gravity anomaly data obtained from the GGMplus model, which provides ultra-high-resolution gravity field estimates at ~200 m spatial resolution (Hirt et al. 2013). These data make it easy to access without requiring large costs when compared to direct surveys. The study area is located within the Palu region, Central Sulawesi, Indonesia, covering the coordinates 0.8° – 1.2° S and 119.7° – 120.0° E (Fig. 1b). The gravity data used in this study consist of free-air anomaly (FAA) values sourced from the gravity data folder (ga) of GGMplus (https://ddfe.blazejbucha.com/models/GGMplus/data/ga/). Additionally, topographic data for Bouguer correction and terrain effect analysis were obtained from the digital elevation model (dg) folder of GGMplus (https://ddfe.blazejbucha.com/models/GGMplus/data/dg/). Importantly, while GGMplus incorporates topographic effects in its gravity modelling, it does not independently generate topographic data but rather integrates external DEM sources such as SRTM, ASTER and EGM2008 (Hirt et al. 2013). This study uses SRTM-derived elevation data at 3 arc-second (~90 m) resolution for terrain corrections in Bouguer anomaly calculations.

The data we used on fracture patterns served as supporting data in this study, as seen in Fig. 1b from Valkaniotis et al. (2018). The location of the fracture pattern can then be compared with the analysis of the derivative processing results that have been carried out to study the subsurface structure of the fracture pattern.

Data processing

The processing of gravity data began with the computation of the Simple Bouguer Anomaly (SBA), which required estimating the average density and applying Bouguer corrections. The Parasnis method (Parasnis and Cook 1952; Ritchie et al. 1966; Rao and Satyanarayana 1973; Gabo et al. 2015; Armada et al. 2020) was used to estimate the average density, assuming that the Bouguer Anomaly value is zero. The Bouguer correction was then calculated using standard formulas, incorporating topographic height variations derived from SRTM-based elevation models (Hirt et al. 2013). The final SBA values were obtained by subtracting the Bouguer correction from the free-air anomaly (FAA) at each grid point, ensuring the removal of terrain-induced gravity effects.

To further refine the gravity anomaly data, anomaly separation was performed using the moving average method (Stanley 1977; Reynolds 1997; Fedi and Florio 2001; Du and Zhang 2021). This approach effectively differentiates regional and residual anomalies, where long-wavelength anomalies related to deep-seated geological structures were filtered out, allowing short-wavelength residual anomalies to be extracted for more precise fault identification. The resulting residual anomalies were then utilised for further geological structure analysis.

Once the SBA and residual anomalies were determined, First Horizontal Derivative (FHD) and Second Vertical Derivative (SVD) analyses were conducted to enhance the identification of subsurface structures. The FHD values were

computed using the first-order finite difference method along the x and y directions to highlight lateral density contrasts, while the SVD values were calculated as the negative of the second-order horizontal derivatives, emphasizing vertical density variations associated with fault structures. These derivative calculations were performed using Microsoft Excel, and the results were visualised as thematic maps with Generic Mapping Tools (GMT) (Wessel et al. 2019).

An essential aspect of the analysis involved addressing the impact of terrain effects on SBA, FHD and SVD results. Since the FAA values obtained from GGMplus inherently include terrain-induced gravity effects, additional residual terrain modelling (RTM) was applied to minimise high-frequency noise (Forsberg 1984; Hirt et al. 2010). The influence of uncorrected terrain effects on gravity-derived fault structures was evaluated by comparing the results with mapped surface rupture patterns from Valkaniotis et al. (2018). This comparison ensured that the gravity-derived fault traces were consistent with observed earthquake-induced surface deformation, thereby improving the reliability of fault identification.

The final step of the data processing involved interpreting the derivative results in relation to geological structures identified in previous studies. The gravity-based fault delineations were cross-referenced against existing fault maps, seismicity records and geological data to assess their accuracy in identifying active fault zones. The integration of gravity anomaly analysis with geological and geophysical constraints provided a comprehensive understanding of subsurface faulting mechanisms, which is crucial for seismic hazard assessment and disaster mitigation. To enhance the clarity and reproducibility of this study, a simplified research flowchart is presented in Figure 2. This diagram outlines the overall methodological framework applied in this research.

Results

Simple Bouguer Anomaly

The SBA (Simple Bouguer Anomaly) value is obtained by making Bouguer corrections to the FAA data. Before obtaining the Bouguer correction value, the average density estimation is first determined using the Parasnis method (Parasnis and Cook 1952; Ritchie et al. 1966; Rao and Satyanarayana 1973; Gabo et al. 2015; Armada et al. 2020). The results obtained for the average density estimation value in this study were 2.5183 gr/cm^3, as shown in Figure 3.

The average density value obtained is then used to determine the Simple Bouguer Anomaly (SBA)

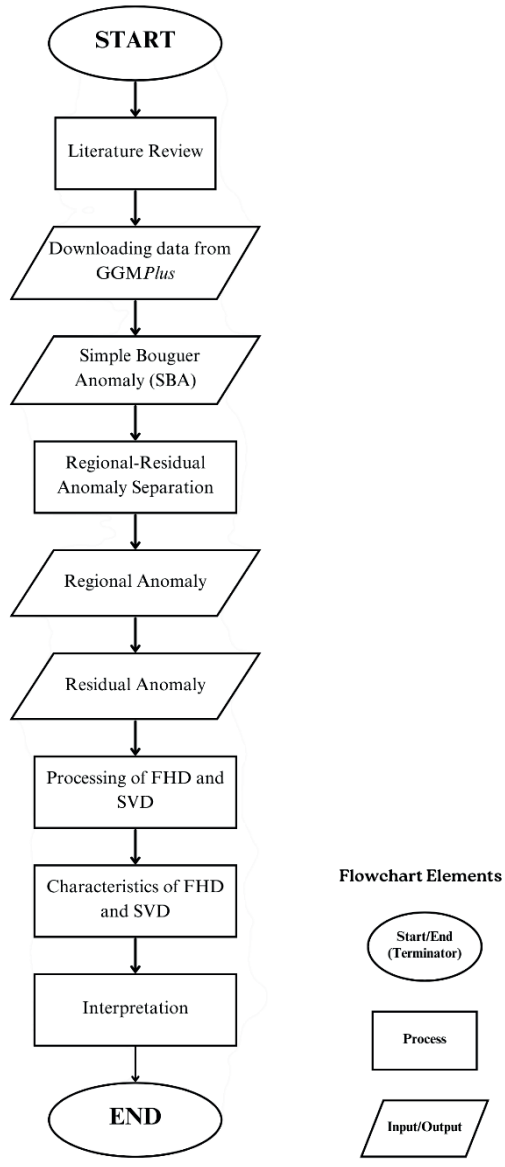

Fig. 2. Research flowchart

value. Then the anomaly distribution mapping of the SBA value in the study area is carried out.

The Simple Bouguer Anomaly (SBA) values obtained in this study range from –2 mGal to 56 mGal, highlighting significant subsurface density variations in the Palu region (Fig. 4). Lower anomaly values are generally associated with areas of low-density materials, such as sedimentary basins, while higher values indicate denser geological structures (Sunil et al. 2010; Lewerissa et al. 2017; Guglielmetti and Moscariello 2021). Specifically, the Palu-Koro Fault exhibits a pronounced gradient in anomaly values, which is indicative of a sharp contrast in subsurface densities. The anomaly variations align with the tectonic complexity of the region, particularly the northwest–southeast direction of faulting, as previously identified in geological studies (Fig. 1c).

This Simple Bouguer Anomaly value is a combination of values between the residual anomaly (shallow) and regional anomaly (deep), so it is necessary to separate the two anomalies. The purpose of anomaly separation is to determine the source of deep and shallow anomalies (Stanley 1977; Reynolds 1997; Fedi and Florio 2001; Du and Zhang 2021). In this study, separation is used using the moving average method (Stanley 1977; Reynolds 1997; Fedi and Florio 2001; Du and Zhang 2021). This process is assisted by analysing the spectrum to obtain the cut-off wave number used to determine the window width in the moving average process. From the separation results, the regional and residual Bouguer anomaly maps are shown in Figure 5.

The residual anomaly obtained through moving average techniques further clarified the structural details. The regional anomaly map showed smoother, broader patterns, while the residual anomaly map revealed localised density contrasts. This separation provided a clearer understanding of the subsurface features associated with active faulting, such as the Palu-Koro Fault and adjacent surface rupture zones.

Determination of fault types

The study of subsurface structures may produce mixed results, so in this study we used derivative methods (FHD and SVD) to help learn more about the determination of subsurface structures. The calculation of the derivative method (FHD and SVD) is done statistically using equations (3) and (8) with the help of Microsoft Excel software. In areas where there are geological structure boundaries, the First Horizontal Derivative (FHD) of the obtained gravity anomalies tends to have a characteristic maximum or minimum value. Meanwhile, the Second Vertical Derivative (SVD) of the gravity anomaly caused by the geological structure will have a maximum absolute value and a minimum absolute value and is limited by a value of zero or close to zero as the limit of its geological characteristics. The FHD and SVD of the obtained gravity anomalies can be used

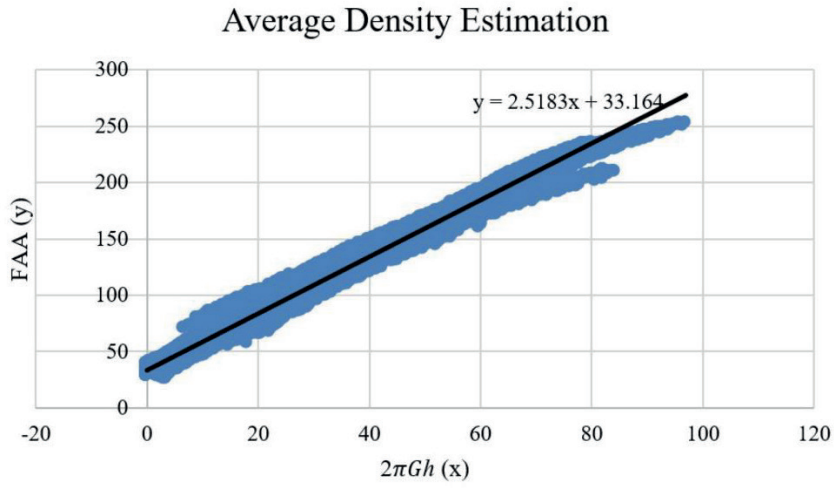

Fig. 3. Application of the Parasnis method for estimating average rock density

Citation: Bulletin of Geography. Physical Geography Series 2025, 28, http://doi.org/10.12775/bgeo-2025-0006

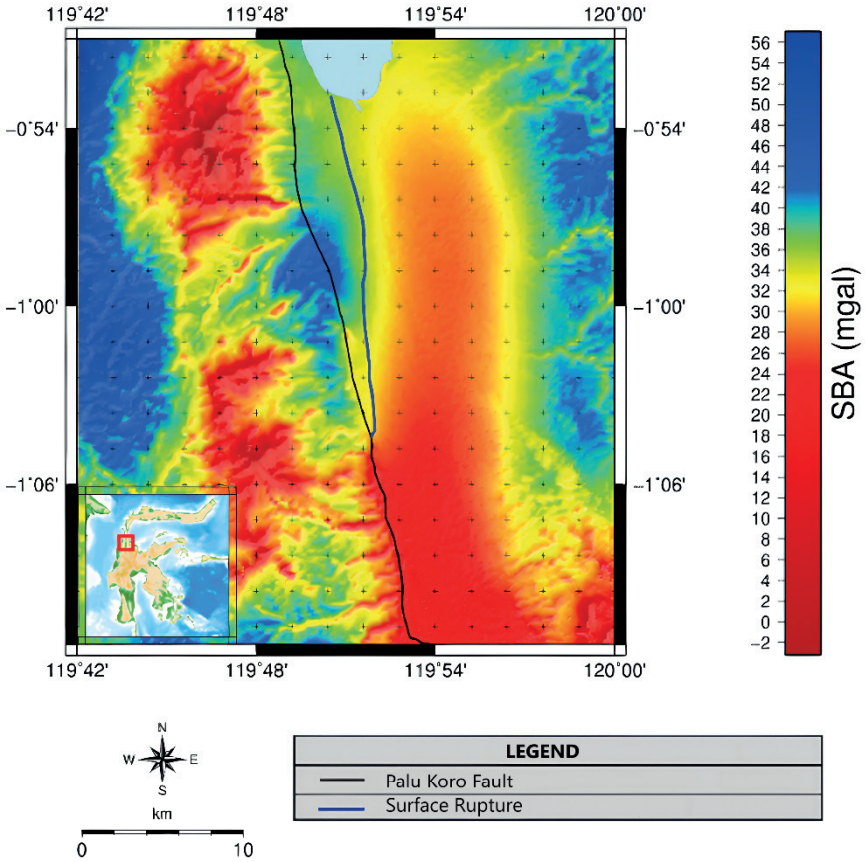

Fig. 4. Simple Bouguer Anomaly (SBA) map of the study area. The map reveals low anomaly zones (–2 to 15 mGal) in the Palu Basin, interpreted as sedimentary fill, and high anomalies (35–56 mGal) in the eastern segments, indicating denser crustal blocks likely related to basement structures.

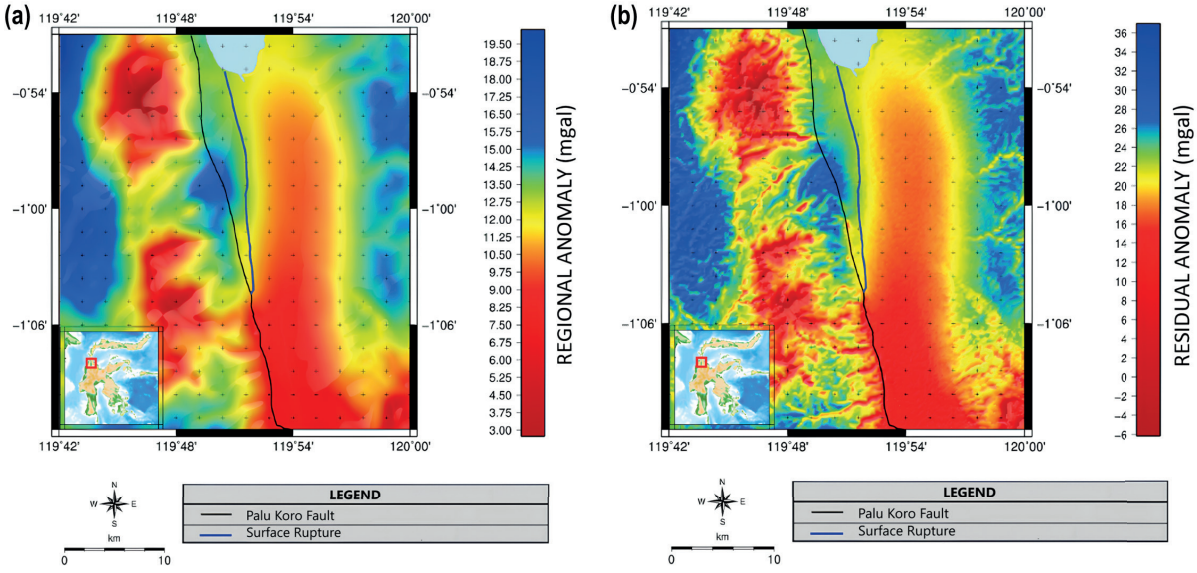

Fig. 5. Gravity anomaly separation using moving average filtering. (a) Regional anomaly map showing broad trends of crustal uplift and subsidence; (b) Residual anomaly map highlighting localised density contrasts, particularly along the Palu-Koro Fault trace

to determine the type of fault by geological sections of the fault to be determined.

In this study, no fixed numerical threshold was applied for delineating fault segments from the FHD and SVD profiles. Instead, the process involved a qualitative and empirical approach, based on identifying prominent local maxima and minima, as well as zero crossings, in the derivative profiles. On FHD curves, fault boundaries are typically associated with peaks (positive or negative) that mark high-density lateral contrasts. On SVD profiles, fault structures are often identified by zero-crossing points, where the sign of the second derivative changes, indicating vertical density discontinuities. These features were visually inspected and interpreted across all 11 cross-sections (Figs 6 and 7). Although the numerical values of SVD commonly fall within a narrow range (approximately 0.00001–0.0001), the interpretation focused on relative contrasts rather than fixed cut-offs. The interpreted segments were then validated through spatial alignment with surface rupture maps, relocated seismicity, and InSAR-derived slip distributions (Fang et al. 2019; Supendi et al. 2019; Natawidjaja et al. 2021). This combined visual–empirical approach aligns with established gravity interpretation techniques (Bott 1962; Sarkowi et al. 2010; Sumintadireja et al. 2018).

The Palu-Koro Fault and surface rupture are suspected to be located in the surroundings of Palu Bay. Therefore, 11 sections (Fig. 6) were made along the border of the study area to determine the type of fault on the Palu Fault and surface rupture.

The sections shown in Figure 6 are used to analyse the graph of FHD-SVD values displayed in the form of a scatter graph. The analysis of the FHD-SVD graph is an indicator in determining the type of Palu Fault and also the rupture surface in the study area. Based on the FHD-SVD value graph, the FHD values of the gravity anomaly in both the Palu-Koro Fault incision and the surface rupture mostly show sharp characteristics in the form of minimum or maximum anomaly values. However, in the B-B', E-E' and F-F' sections, the results obtained do not show any sharp characteristics of the anomalous values. From all the results of the FHD sections that have been made on the Palu-Koro Fault and also the rupture surface, they have a correlation with the zero value on the SVD value graph. Therefore, it can be classified that there is a geological structure boundary in the sections area.

The SVD analysis for the Palu-Koro Fault shows that nine of the geological sections have absolute maximum values greater than their corresponding absolute minimum values, while two sections exhibit

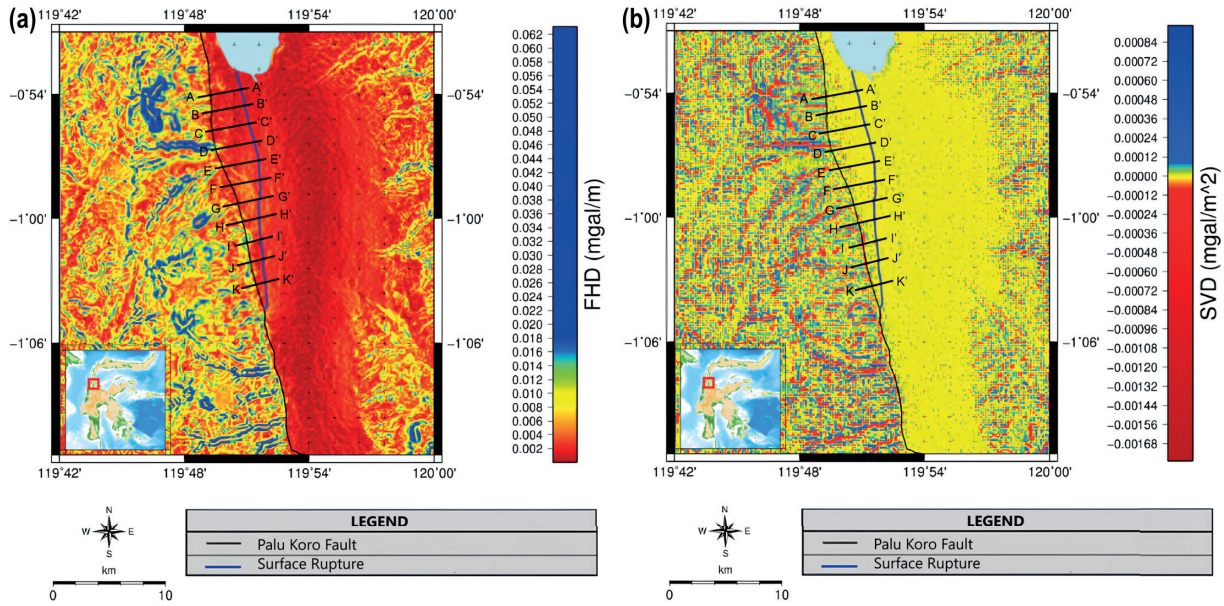

Fig. 6. First Horizontal Derivative (FHD) and Second Vertical Derivative (SVD) maps. (a) FHD reveals lateral density contrasts useful for detecting fault boundaries; (b) SVD highlights vertical density gradients that correlate with known surface ruptures and seismicity

Citation: Bulletin of Geography. Physical Geography Series 2025, 28, http://doi.org/10.12775/bgeo-2025-0006

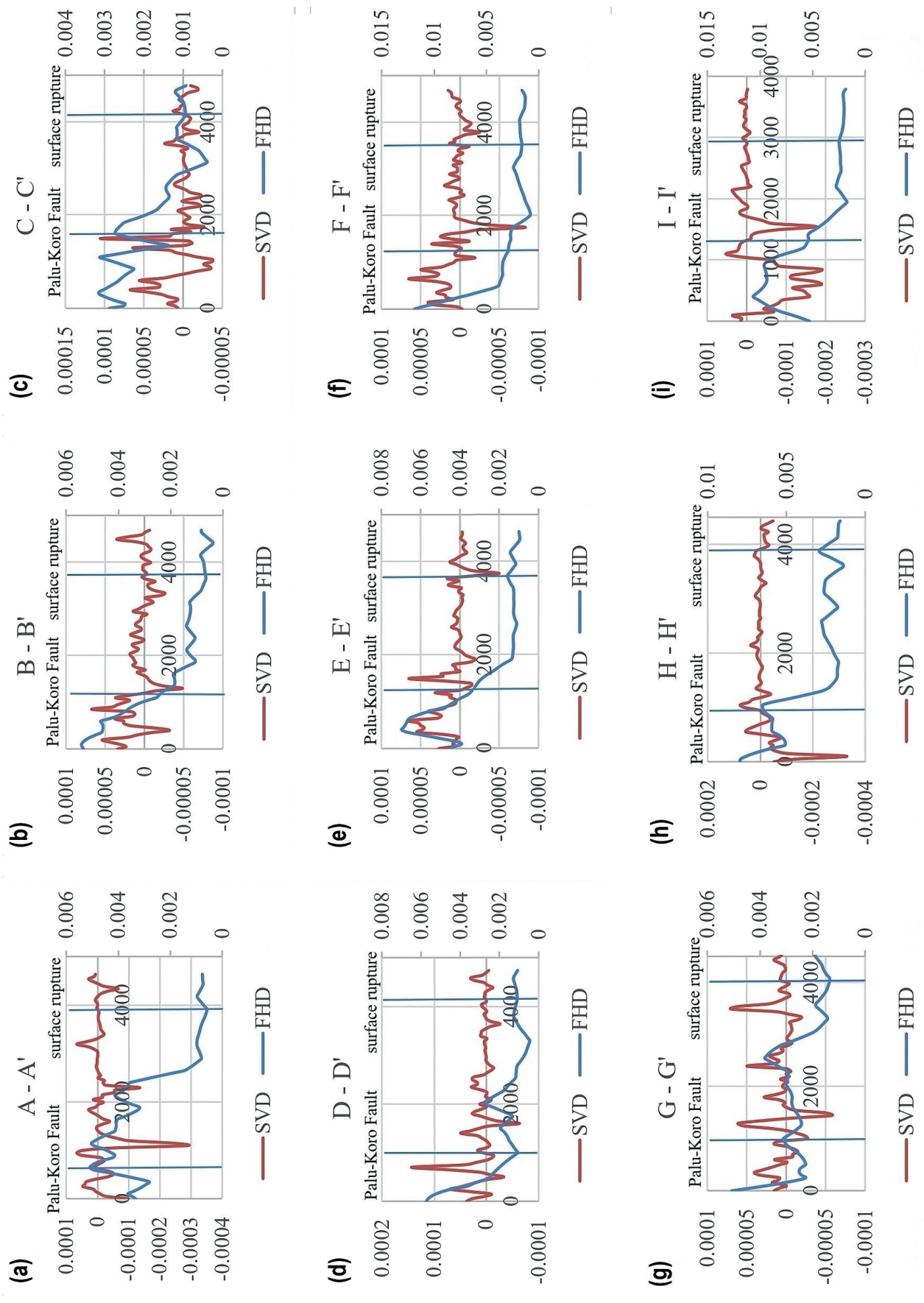

Fig. 7. Continued on the following page

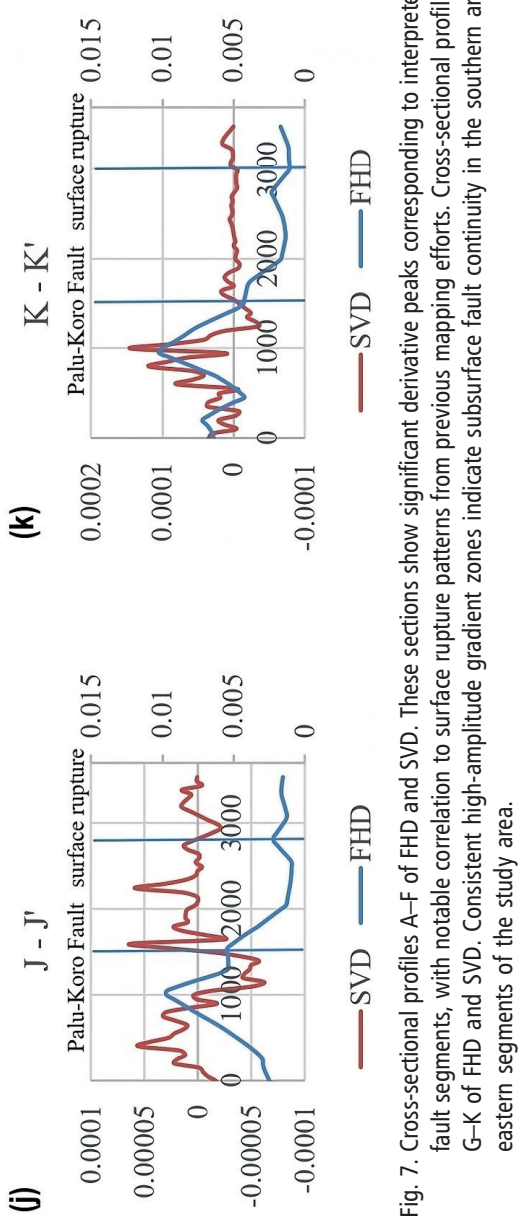

Fig. 7. Cross-sectional profiles A–F of FHD and SVD. These sections show significant derivative peaks corresponding to interpreted fault segments, with notable correlation to surface rupture patterns from previous mapping efforts. Cross-sectional profiles G–K of FHD and SVD. Consistent high-amplitude gradient zones indicate subsurface fault continuity in the southern and eastern segments of the study area.

absolute maximum values smaller than their absolute minimum values (Table 1 and Fig. 7). In contrast, the SVD analysis for the surface rupture indicates that seven of the 11 sections possess absolute maximum values exceeding their absolute minimum values, whereas the remaining four sections show higher absolute minimum values compared to their absolute maximum values.

According to the SVD criteria outlined in Equations (9), (10) and (11), the nine sections along the Palu-Koro Fault can be classified as strike-slip faults with slight downward motion. Meanwhile, two sections, namely B–B' and K–K', are categorised as strike-slip faults with slight upward motion. For the surface rupture, seven sections are identified as strike-slip faults with minor downward motion, while the other four sections, specifically A–A', E–E', G–G' and K–K', are classified as strike-slip faults with slight upward motion.

Based on the analysis of 11 sections along the Palu-Koro Fault and the surface rupture, nine sections of the Palu-Koro Fault exhibit strike-slip faulting with minor downward displacement, and two sections show strike-slip faulting with slight upward displacement. Similarly, the surface rupture analysis reveals seven sections as strike-slip faults with minor downward motion, whereas four sections are classified as strike-slip faults with slight upward motion. These findings suggest that the Palu-Koro Fault predominantly functions as a strike-slip fault with slight downward displacement. Moreover, the surface rupture in the study area is assumed to have resulted from the same strike-slip mechanism with minor downward motion.

The fault responsible for the surface rupture is likely part of the same segment as the Palu-Koro Fault, as indicated by the proximity of the surface rupture to the fault and the similarity in FHD-SVD patterns. This correlation confirms that the surface rupture was caused by fault activity in Palu City, with a northwest–southeast orientation. The mapping of surface rupture paths, supported by this analysis, provides a valuable reference for disaster mitigation and the development of hazard-prone zone maps.

Discussion

The results of this study highlight the effectiveness of Simple Bouguer Anomaly (SBA) analysis

Citation: Bulletin of Geography. Physical Geography Series 2025, 28, http://doi.org/10.12775/bgeo-2025-0006

Table 1. SVD values of geological sections

Cross-sections	SVD Value of Palu-Koro Fault		SVD Value of surface rupture	
	Absolute Minimum	Absolute Maximum	Absolute Minimum	Absolute Maximum
A-A'	0.0000226	0.0000512	0.0000036	0.0000019
B-B'	0.0000486	0.0000372	0.0000029	0.0000033
C-C'	0.0000099	0.0000173	0.0000096	0.0000127
D-D'	0.0000139	0.0000158	0.0000014	0.0000037
E-E'	0.0000147	0.0000317	0.0000146	0.0000129
F-F'	0.0000112	0.0000247	0.0000112	0.0000131
G-G'	0.0000574	0.0000612	0.0000034	0.0000076
H-H'	0.00004	0.0000758	0.0000335	0.0000187
I-I'	0.0000097	0.0000185	0.0000075	0.0000108
J-J'	0.0000572	0.0000632	0.0000009	0.0000021
K-K'	0.0000246	0.0000142	0.0000055	0.0000013

and derivative techniques (FHD and SVD) in delineating fault structures and characterising subsurface dynamics in the tectonically complex Palu region. The SBA values, ranging from –2 to 56 mGal, reveal significant density variations within the subsurface, where lower values correspond to sedimentary basins, whereas higher values indicate denser geological formations (Sukamto 1982; Sunil et al. 2010; Lewerissa et al. 2017; Guglielmetti and Moscariello 2021; Natawidjaja et al. 2021). These findings align with the established geological framework of Sulawesi, which is characterised by active fault systems, particularly the Palu-Koro Fault (Sukamto 1982; Bellier et al. 2001; Watkinson 2011; Natawidjaja et al. 2021).

The gravity anomaly gradients identified in this study correspond well with hypocentre relocation studies from Supendi et al. (2019, 2020) and Global Centroid Moment Tensor (GCMT) solutions (Ekström et al. 2012), which identified a NW–SE trending aftershock sequence following the 2018 Mw 7.5 Palu earthquake. The alignment between seismic activity and subsurface density contrasts suggests a structural link between fault segmentation and rupture propagation (Daryono 2016; Valkaniotis et al. 2018, Natawidjaja et al. 2021). Further supporting this hypothesis, double-difference relocation results (Supendi et al. 2019, 2020) show that most aftershocks occurred along the eastern side of the Palu-Koro Fault, at depths shallower than 20 km, reinforcing the interpretation that the fault system is structurally complex.

The findings of this study are further validated by InSAR-derived coseismic deformation patterns (Fang et al. 2019), which indicate that the 2018 earthquake propagated at supershear velocity (~4.1 km/s). This high rupture speed, along with the presence of multiple slip asperities, suggests that the Palu-Koro Fault is highly segmented. The four major slip asperities identified in the InSAR study correspond to areas of significant density contrast in the SBA and residual anomaly maps, reinforcing the fault segmentation model proposed by Natawidjaja et al. (2021). Specifically, Fang et al. (2019) reported a maximum coseismic slip of ~6.5 metres in the southern segment of the fault, which aligns spatially with the most prominent residual gravity anomaly and sharp SVD gradients observed in this study. Although we did not reproduce their slip distribution figure due to data access limitations and authorship considerations, spatial comparisons were made using published maps, providing a semi-quantitative validation of the gravity-derived segmentation. The integration of gravity data with InSAR observations strengthens the argument that density contrasts identified through SBA and SVD analysis can effectively delineate rupture-prone segments of the fault.

The regional and residual anomaly separation provided further clarity on subsurface structures, with residual anomalies capturing localised density contrasts that are consistent with mapped fault traces

(Fedi and Florio 2001; Du and Zhang 2021; Sarkowi et al. 2022). The sharp residual anomaly gradients along the Palu-Koro Fault indicate well-defined geological boundaries, which align with seismic relocation studies (Supendi et al. 2019, 2020) and geological fault mapping (Sukamto 1982; Natawidjaja et al. 2021). The derivative analysis (FHD and SVD) further refined fault boundary delineation, with FHD highlighting lateral discontinuities and SVD capturing vertical density variations. The Palu-Koro Fault is predominantly left-lateral strike-slip, but localised vertical displacement (e.g., in segments B–B' and K–K') suggests structural complexities within the fault system. This observation correlates well with previous studies that identified multi-segment rupture behaviour, fault bends and pull-apart basins (Daryono 2016; Supendi et al. 2019; Natawidjaja et al. 2021).

These interpretations are further supported by recent studies that explore the relationship between gravity anomalies, fault segmentation and seismic activity along the Palu-Koro Fault system. Hanif et al. (2024) and Patria et al. (2023) demonstrated that lithospheric thinning and variations in fault slip rate – derived from gravity modelling – strongly correlate with local subsurface complexity and rupture behaviour. Gravity anomalies were shown to correspond with deep basement structures and potential rupture zones, consistent with findings in this study. In addition, Putrie and Husein (2024) applied focal mechanism analysis to map fault plane geometry, which aligned with gravity-defined segments. These independent datasets reinforce that gravity-based techniques, especially when integrated with seismic data, offer reliable insights into the segmentation, stress accumulation and rupture potential of active faults in Central Sulawesi (Bao et al. 2019; Jayadi et al. 2023; Rosid 2023).

In addition to structural and seismological validations, the lithological characteristics along the Palu-Koro Fault also support the gravity-based interpretations presented in this study. The fault system traverses a geologically diverse region composed of sedimentary, volcanic and metamorphic units formed through long-term tectonic processes (Polcari et al. 2019; Wang et al. 2019; Hanif et al. 2024). Variations in lithology – such as young volcanic rocks, marine sediments and reactivated thrust zones – affect subsurface density distributions, which are captured as gravity anomalies in the SBA, FHD and SVD results. These geological contrasts contribute to the spatial heterogeneity of seismic behaviour along the fault, including the propagation of the 2018 supershear rupture (Bao et al. 2019; Li et al. 2022; Jayadi et al. 2023). Integrating lithological context with gravity and seismic data thus enhances the reliability of fault segmentation analysis and provides critical insights for hazard assessment in Palu and surrounding regions (Jaya et al. 2019; Syamsuddin et al. 2024).

While SVD analysis effectively delineates fault boundaries, its application in fault classification remains debated. Sumintadireja et al. (2018) emphasised that SVD alone cannot reliably determine fault kinematics, as density variations may be influenced by non-tectonic factors, including lithological contrasts and sediment compaction. In this study, the assumption that the relative intensities of second vertical derivative peak values can be used to classify normal, reverse and strike-slip faults is adapted from Bott (1962), which was originally developed for granitic intrusions and sedimentary basins. However, as Sumintadireja et al. (2018) suggests, caution must be exercised when applying this method to complex fault systems like Palu-Koro, where fault behaviour is influenced by regional stress fields and local geological heterogeneities. These findings highlight the need to integrate SVD analysis with seismic and geological data to improve fault classification accuracy and avoid misinterpretations.

Additionally, terrain effects on gravity anomaly analysis could introduce minor biases in fault structure delineation due to the lack of explicit terrain corrections in this study. High-resolution topographic corrections have been shown to significantly improve gravity anomaly accuracy in regions with rugged terrain (Sembiring et al. 2023; Godah et al. 2024). Although the Palu region exhibits moderate elevation variations, some residual terrain effects may still be present in the FHD and SVD results, potentially influencing fault interpretations (Gunawan and Permana 2024). However, the alignment between gravity-derived fault segments, InSAR coseismic deformation and seismic aftershock distributions suggests that these effects have not significantly distorted the structural interpretations. Future research should incorporate higher-resolution DEM-based terrain corrections to refine gravity anomaly processing and further improve fault mapping accuracy (Pavlis et al. 2012; Ruiyin et al. 2024).

These findings have significant implications for seismic hazard assessment and urban planning in Palu City and surrounding areas. The correlation between gravity anomalies, surface rupture patterns and aftershock distributions suggests the potential for future fault activity along previously unmapped segments. As indicated by Natawidjaja et al. (2021), the multi-segment nature of the Palu-Koro Fault implies that future earthquakes could rupture different fault strands, increasing uncertainty in seismic hazard prediction. The geophysical results of this study further confirm that surface ruptures tend to remain within the extent of the fault plane (Schwartz and Coppersmith 1984; Mankhemthong et al. 2012), but, in some cases, rupture propagation may extend beyond mapped faults when strain energy release exceeds fault plane limitations (Wells and Coppersmith 1994; Eshaghzadeh et al. 2015; Natawidjaja et al. 2021). Therefore, areas near the fault zone should remain vigilant, as secondary ruptures could develop during future seismic events (Xu et al. 2008; Liang et al. 2021; Purba et al. 2024).

To further refine fault models and seismic hazard assessments, future research should focus on incorporating additional geophysical methods such as seismic tomography for deeper fault structure imaging (Biryol et al. 2013), seismic relocation techniques to enhance hypocentre accuracy (Waldhauser and Schaff 2007), and LiDAR drone systems for high-resolution surface rupture mapping (Chen et al. 2015). The integration approaches further improve the classification of fault structures and enhance earthquake risk assessment strategies (Eppelbaum et al. 2020; Umar 2023; Purba et al. 2025).

In conclusion, this study reinforces the importance of gravity-based geophysical methods in fault characterisation, particularly in complex strike-slip systems like Palu-Koro. By correlating gravity anomalies with seismic, InSAR and geological data, this research provides a comprehensive understanding of subsurface faulting mechanisms. The integration of SBA, FHD and SVD techniques with previous seismic relocation studies (Supendi et al. 2019, 2020), InSAR (Fang et al. 2019), and geological study (Sukamto 1982; Sunil et al. 2010; Lewerissa et al. 2017; Daryono 2016; Guglielmetti and Moscariello 2021; Natawidjaja et al. 2021) confirms that the Palu-Koro Fault is highly segmented, with variations in rupture dynamics and surface expression. These insights contribute to disaster mitigation planning and the development of resilience strategies for earthquake-prone regions. The demonstrated effectiveness of derivative-based gravity analysis highlights its potential for further integration with other geophysical methods, ensuring a more robust and reliable approach to seismic hazard assessment and fault mapping in tectonically active zones.

Conclusion

This study demonstrates the effectiveness of gravity anomaly analysis – specifically Simple Bouguer Anomaly (SBA), First Horizontal Derivative (FHD) and Second Vertical Derivative (SVD) – in delineating fault structures along the Palu-Koro Fault in Central Sulawesi. These techniques reveal distinct density contrasts and structural discontinuities, which correspond spatially with mapped surface ruptures, relocated seismicity and InSAR-derived deformation. The integration of residual and derivative gravity maps provides enhanced resolution of fault segmentation, including strike-slip and localised vertical displacements, consistent with previous geological and seismological studies.

Importantly, the correlation between gravity anomalies and slip asperities from the 2018 Mw 7.5 Palu earthquake validates the use of gravity-based methods in identifying rupture-prone segments. These findings confirm that derivative-based gravity analysis can effectively characterise fault complexity in regions with limited surface exposure or incomplete geological mapping.

From a practical perspective, the study provides actionable insights for seismic hazard assessment and urban planning in Palu City and surrounding areas. By identifying high-risk fault segments with potential for complex rupture behaviour, this research supports the development of more targeted earthquake mitigation strategies. The methodology presented here also offers a cost-effective and replicable framework for fault analysis in other tectonically active regions. Future work should integrate additional geophysical datasets – such as seismic tomography, hypocentre relocation and LiDAR-based surface mapping – to further improve fault characterisation and strengthen regional disaster preparedness.

Acknowledgment

The authors would like to thank the Meteorology, Climatology and Geophysics Agency, especially the team from the Gowa Geophysical Station, for helping to complete this research. The authors would also like to thank the International Gravimetric Bureau for providing freely accessible gravity data. We would like to express our sincere gratitude to the two anonymous reviewers for their valuable comments and constructive suggestions, which have greatly contributed to improving the quality of this paper.

Disclosure statement

No potential conflict of interest was reported by the authors.

Author contributions

Study design: MF, PA, JP; data collection: MF, TMA, PA; statistical analysis: MF, TMA, JP; result interpretation: MF, JP, PA; manuscript preparation: JP, MF; literature review: JP, MF.

References.

ANDRIAMAMONJISOA SN and HUBERT-FERRARI A, 2019, Combining geology, geomorphology and geotechnical data for a safer urban extension: Application to the Antananarivo capital city (Madagascar). *Journal of African Earth Sciences* 151: 417-437. DOI: https://doi.org/10.1016/j.jafrearsci.2018.12.003.

ARMADA L, DIMALANTA C, PARCUTELA N, AUSTRIA R, PADRONES J, PAYOT B, QUEAÑO K and YUMUL G, 2020, Bouguer Anomaly of Central Cebu, Philippines. *Journal of Maps* 16(2): 577-584. DOI: https://doi.org/10.1080/17445647.2020.1791270.

BAO H, AMPUERO J, MENG L, FIELDING E J, LIANG C, MILLINER C, HUANG H and others, 2019, Early and persistent supershear rupture of the 2018 magnitude 7.5 Palu earthquake. *Nature Geoscience* 12(3): 200–205. DOI: https://doi.org/10.1038/s41561-018-0297-z.

BELLIER O, SIAME L, BEAUDOUIN T, VILLENEUVE M and BRAUCHER R, 2001, High slip rate for a low seismicity along the Palu-Koro active fault in Central Sulawesi (Indonesia). Terra Nova 13(6): 463-470. DOI: https://doi.org/10.1046/j.1365-3121.2001.00382.x.

BIASI GP and WESNOUSKY SG, 2016, Steps and gaps in ground ruptures: Empirical bounds on rupture propagation. *Bulletin of the Seismological Society of America*, 106(3): 1110-1124. DOI: https://doi.org/10.1785/0120150175.

BIRYOL CB, LEAHY GM, ZANDT G and BECK SL, 2013, Imaging the shallow crust with local and regional earthquake tomography. *Journal of Geophysical Research: Solid Earth* 118(5): 2289-2306. DOI: https://doi.org/10.1002/jgrb.50115.

BLAKELY J, 1995, *Potential Theory in Gravity and Magnetic Applications*. Cambridge University Press. DOI: https://doi.org/10.1017/cbo9780511549816.

BMKG, 2019, Indonesian Tsunami Catalog 416-2018. Center for Earthquake and Tsunami, Deputy for Geophysics (in Indonesian).

BMKG, 2023, Indonesian Earthquake Catalog: Hypocenter Relocation and Tectonic Implications. Center for Earthquake and Tsunami, Deputy for Geophysics (in Indonesian)

BNPB, 2019, Damage and impact of disaster in Central Sulawesi (in Indonesian). Available at: https://www.bnpb.go.id/kerugian-dan-kerusakan-dampak-bencana-di-sulawesi-tengah-mencapai-1382-trilyun-rupiah.

BOTT M H P, 1962, A simple criterion for interpreting negative gravity anomalies. Geophysics 27(3). DOI: https://doi.org/10.1190/1.1439026

BURGER HR, SHEEHAN AF and JONES CH, 2023, Exploration using gravity. In: Introduction to Applied Geophysics. Cambridge University Press. DOI: https://doi.org/10.1017/9781009433112.008.

CHEN T, AKCIZ SO, HUDNUT KW, ZHANG DZ and STOCK JM, 2015, Fault-slip distribution of the 1999 Mw 7.1 Hector mine earthquake, California, estimated from postearthquake airborne LiDAR data. *Bulletin of the Seismological Society of America* 105(2): 776-790. DOI: https://doi.org/10.1785/0120130108.

CHENG Y, ALLEN RM and TAIRA T, 2023, A new focal mechanism calculation algorithm (REFOC) using inter-event relative radiation patterns: Application to the earthquakes in the Parkfield Area. *Journal of Geophysical*

Research: Solid Earth 128(3): e2022JB025006. DOI: https://doi.org/10.1029/2022JB025006.

DARYONO MR, 2016, *Paleoseismology of Tropical Indonesia (Case study in Sumatran Fault, Palukoro-Matano Fault, and Lembang Fault)*. Dissertation, Earth Science Doctoral Programme, Institut Teknologi Bandung.

DEWANTO BG, PRIADI R, HELIANI LS, NATUL AS, YANIS M, SUHENDRO I and JULIUS AM, 2022, The 2022 Mw 6.1 Pasaman Barat, Indonesia earthquake, confirmed the existence of the Talamau Segment Fault based on teleseismic and satellite gravity data. *Quaternary* 5(4): 45. DOI: https://doi.org/10.3390/quat5040045.

DU W and ZHANG Y, 2021, The calculation of high-order vertical derivative in gravity field by Tikhonov regularization iterative method. *Mathematical Problems in Engineering* 2021(1): 8818552. DOI: https://doi.org/10.1155/2021/8818552.

EKSTRÖM G, NETTLES M and DZIEWOŃSKI AM, 2012, The global CMT project 2004–2010: Centroid-moment tensors for 13,017 earthquakes. *Physics of the Earth and Planetary Interiors* 200: 1-9. DOI: https://doi.org/10.1016/j.pepi.2012.04.002.

ELKINS TA, 1951, The second derivative method of gravity interpretation. *Geophysics* 16(1): 29-50. DOI: https://doi.org/10.1190/1.1437648.

EPPELBAUM L, BEN-AVRAHAM Z, KATZ Y, CLOETINGH S and KABAN M, 2020, Combined multifactor evidence of a giant lower-mantle ring structure below the Eastern Mediterranean. *Positioning* 11(2): 11-32. DOI: https://doi.org/10.4236/pos.2020.112002.

ESHAGHZADEH A, KALANTARI RS and MOEINI HEKMAT Z, 2015, Optimum density determination for Bouguer correction using statistical methods: A case study from north of Iran. *International Journal of Advanced Geosciences* 3(2): 25-29. DOI: https://doi.org/10.14419/ijag.v3i2.4988.

FANG J, XU C, WEN Y, WANG S, XU G, ZHAO Y and YI L, 2019, The 2018 Mw 7.5 Palu earthquake: A supershear rupture event constrained by InSAR and broadband regional seismograms. *Remote Sensing* 11(11): 1330. DOI: https://doi.org/10.3390/rs11111330.

FEDI M and FLORIO G, 2001, Detection of potential fields source boundaries by enhanced horizontal derivative method. *Geophysical Prospecting* 49(1): 40–58. DOI: https://doi.org/10.1046/j.1365-2478.2001.00235.x.

FORSBERG R, 1984, *A study of terrain reductions, density anomalies and geophysical inversion methods in gravity field modelling*. Danish Geodetic Institute.

GABO JAS, DIMALANTA CB, YUMUL GP, FAUSTINO-ESLAVA DV and IMAI A, 2015, Terrane boundary geophysical signatures in Northwest Panay, Philippines: Results from gravity, seismic refraction and electrical resistivity investigations. *Terrestrial, Atmospheric and Oceanic Sciences* 26(6). DOI: https://doi.org/10.3319/TAO.2015.05.11.03(TC).

GODAH W, SZELACHOWSKA M and GEDAMU AA, 2024, Accuracy assessment of high and ultra-high-resolution combined GGMs, and recent satellite-only GGMs – Case studies of Poland and Ethiopia. *Reports on Geodesy and Geoinformatics* 117(1): 38–44. DOI: https://doi.org/10.2478/rgg-2024-0005.

GUGLIELMETTI L and MOSCARIELLO A, 2021, On the use of gravity data in delineating geologic features of interest for geothermal exploration in the Geneva Basin (Switzerland): Prospects and limitations. *Swiss Journal of Geosciences* 114(1): 1-20. DOI: https://doi.org/10.1186/s00015-021-00392-8.

GUNAWAN B and PERMANA N R, 2024, Estimations of the geothermal energy potential in the Mount Anak Krakatau region based on derivative analysis and 3D model of gravitational satellite data. *Indonesian Journal of Energy* 7(1). DOI: https://doi.org/10.33116/ije.v7i1.186.

HALL R, 2002, Cenozoic geological and plate tectonic evolution of SE Asia and the SW Pacific: Computer-based reconstructions, model and animations. *Journal of Asian Earth Sciences* 20(4): 353-431. DOI: https://doi.org/10.1016/S1367-9120(01)00069-4.

HANIF M, HANDAYANI L, PUJI A R, PATRIA A and RAMDHAN M, 2024, Gravity modelling insights into crustal structure: Moho depth and subsurface structures in Central Sulawesi. *IOP Conference Series: Earth and Environmental Science* 1373(1): 012050. DOI: https://doi.org/10.1088/1755-1315/1373/1/012050.

HIRAMATSU Y, SAWADA A, KOBAYASHI W, ISHIDA S and HAMADA M, 2019, Gravity gradient tensor analysis to an active fault: A case study at the Togi-gawa Nangan fault, Noto Peninsula, central Japan. *Earth, Planets and Space* 71(1): 1-8. DOI: https://doi.org/10.1186/s40623-019-1088-5.

HIRT C, 2010, Prediction of vertical deflections from high-degree spherical harmonic synthesis and residual terrain model data. *Journal of Geodesy* 84(3): 179-190. DOI: https://doi.org/10.1007/s00190-009-0354-x.

HIRT C, CLAESSENS S, FECHER T, KUHN M, PAIL R and REXER M, 2013, New ultrahigh-resolution picture of Earth's gravity field. *Geophysical Research Letters* 40(16): 4279-4283. DOI: https://doi.org/10.1002/grl.50838.

IRSYAM M, CUMMINS PR, ASRURIFAK M, FAIZAL L, NATAWIDJAJA DH, WIDIYANTORO S, MEILANO I, TRIYOSO W, RUDIYANTO A, HIDAYATI S, RIDWAN M, HANIFA NR and SYAHBANA AJ, 2020, Development of the 2017 national seismic hazard maps of Indonesia. *Earthquake Spectra* 36(1): 112-136. DOI: https://doi.org/10.1177/8755293020951206.

JAYADI H, SANTOSA BJ, WARNANA DD, ZULFAKRIZA Z, JAMRONI R, SUPENDI P, ROSALIA S, MUTTAQY F, RACHMAN G, PUTRA AS, WIJAYA AD and MEIDJI IU, 2023, A preliminary tomography inversion study on the Palu-Koro Fault, Central Sulawesi using BMKG seismic network. *IOP Conference Series: Earth and Environmental Science* 1227(1): 012032. DOI: https://doi.org/10.1088/1755-1315/1227/1/012032.

KHALID P, BAJWA A A, NAEEM M and DIN Z U, 2016, Seismicity distribution and focal mechanism solution of major earthquakes of northern Pakistan. *Acta Geodaetica et Geophysica* 51(3): 347-357. DOI: https://doi.org/10.1007/s40328-015-0130-8.

KHOGALI A, CHAVANIDIS K, KIRMIZAKIS P, STAMPOLIDIS A and SOUPIOS P, 2024, Reconstruction of the subsurface of Al-Hassa Oasis using gravity geophysical data. *Applied Sciences* 14(9): 3707. DOI: https://doi.org/10.3390/app14093707.

LAYADE G O, EDUNJOBI H, MAKINDE V and BADA B, 2020, Estimation of depth to Bouguer anomaly sources using Euler deconvolution techniques. *Materials and Geoenvironment* 67(4). DOI: https://doi.org/10.2478/rmzmag-2020-0016.

LEWERISSA R, SISMANTO S, SETIAWAN A and PRAMUMIJOYO S, 2018, The study of geological structures in Suli and Tulehu geothermal regions (Ambon, Indonesia) based on gravity gradient tensor data simulation and analytic signal. *Geosciences* (Switzerland) 8(1): 4. DOI: https://doi.org/10.3390/geosciences8010004.

LI C, LIU J, MA J, GANG S, LAN J, LI X, RAN H and others, 2022, Field observations of surface ruptures accompanying a tsunami and supershear earthquake along a plate boundary strike-slip fault. *Geological Magazine* 159(6): 893–903. DOI: https://doi.org/10.1017/s0016756822000012.

LIANG Z, WEI Z, SUN W and ZHUANG Q, 2021, Surface slip distribution and earthquake rupture model of the Fuyun Fault, China, based on high-resolution topographic data. *Lithosphere* 2021(2): 7913554. DOI: https://doi.org/10.2113/2021/7913554.

MANKHEMTHONG N, DOSER DI and BAKER MR, 2012, Practical estimation of near-surface bulk density variations across the Border Ranges Fault System, Central Kenai Peninsula, Alaska. *Journal of Environmental and Engineering Geophysics* 17(3): 151-158. DOI: https://doi.org/10.2113/JEEG17.3.151.

MURDAPA F, SUMANJAYA E, FADLI DI, PERMANA NR, SARI A and PURQAN A, 2024, Optimization of GGMPlus gravity data to identify Sumatran faults segments in Kaba stratovolcano, Bengkulu, revealed by FHD and SVD techniques. *IOP Conference Series: Earth and Environmental Science* 1418(1): 012056. DOI: https://doi.org/10.1088/1755-1315/1418/1/012056.

NATAWIDJAJA DH, DARYONO MR, PRASETYA G, UDREKH, LIU PLF, HANANTO ND, KONGKO W, TRIYOSO W, PUJI AR, MEILANO I, GUNAWAN E, SUPENDI P, PAMUMPUNI A, IRSYAM M, FAIZAL L, HIDAYATI S, SAPIIE B, KUSUMA MA and TAWIL S, 2021, The 2018 Mw7.5 Palu "supershear" earthquake ruptures geological fault's multisegment separated by large bends: Results from integrating field measurements, LiDAR, swath bathymetry and seismic-reflection data. *Geophysical Journal International* 224(2): 985-1002.. DOI: https://doi.org/10.1093/gji/ggaa498.

PARASNIS DS and COOK AH, 1952, A study of rock densities in the English Midlands. Geophysical Journal International 6: 252-271.. DOI: https://doi.org/10.1111/j.1365-246X.1952.tb03013.x.

PATRIA A, PUJI AR and TSUTSUMI H, 2023, Neotectonics of the eastern Matano Fault, Sulawesi, Indonesia: Preliminary results. *IOP Conference Series: Earth and Environmental Science* 1227(1): 012001. DOI: https://doi.org/10.1088/1755-1315/1227/1/012001.

PAVLIS NK, HOLMES SA, KENYON SC and FACTOR JK, 2012, The development and evaluation of the Earth Gravitational Model 2008 (EGM2008). *Journal of Geophysical Research: Solid Earth* 117(4). DOI: https://doi.org/10.1029/2011JB008916.

PHILLIPS JD, 2015, Tools and techniques: Gravitational method. In: Treatise on Geophysics: Second Edition 11. DOI: https://doi.org/10.1016/B978-0-444-53802-4.00197-4.

POLCARI M, TOLOMEI C, BIGNAMI C and STRAMONDO S, 2019, SAR and optical data comparison for detecting co-seismic slip and induced phenomena during the 2018 Mw 7.5 Sulawesi earthquake. *Sensors* 19(18): 3976. DOI: https://doi.org/10.3390/s19183976.

PURBA J, HARISMA H, PRIADI R, AMELIA R, DWILYANTARI AAI, JAYA LMG, RESTELE LO and PUTRA IMWG, 2024, Surface deformation and its implications for land degradation after the 2021 Flores earthquake (M7.4) using differential interferometry synthetic aperture radar. *Journal of Degraded and Mining Lands Management* 12(1): 6819–6831. DOI: https://doi.org/10.15243/jdmlm.2024.121.6819.

PURBA J, RESTELE LO, HADINI LO, USMAN I, HASRIA H and HARISMA H, 2024, Spatial study of seismic hazard using classical probabilistic seismic hazard analysis (PSHA) method in the Kendari City area. *Indonesian Physical Review* 7(3): 300–318. DOI: https://doi.org/10.29303/ipr.v7i3.325.

PURBA J, YULINDA R, PERTIWI II and SAADIA AO, 2025, Seismic hazard analysis in Malang Raya through classical PSHA method using OpenQuake with spatial approach. JAGAT. *Jurnal Geografi Aplikasi dan Teknologi* 9(1): 1–14. DOI: https://doi.org/10.13117/jagat.9.1.1.

PUSGEN, 2017, Indonesia Earthquake Hazard and Source Map 2017. Center for Housing and Settlement Research and Development, Research and Development Agency of the Ministry of Public Works and Housing (PUPR), Jakarta (in Indonesian).

PUSGEN, 2022, Indonesia Earthquake Hazard Deaggregation Map for Earthquake Resistant Infrastructure Planning and Evaluation. Center for Housing and Settlement Research and Development, Research and Development Agency of the Ministry of PUPR, Jakarta (in Indonesian).

PUSGEN, 2024, Indonesia Earthquake Hazard and Source Map 2024. Center for Housing and Settlement Research and Development, Research and Development Agency of the Ministry of PUPR, Jakarta (in Indonesian).

PUTRIE KA and HUSEIN S, 2024, Imaging the fault plane structure of Palu-Koro Fault from earthquake data using Python. *IOP Conference Series: Earth and Environmental Science* 1373(1): 012066. DOI: https://doi.org/10.1088/1755-1315/1373/1/012066.

RAO VB and SATYANARAYANA MURTY BV, 1973, Note on Parasnis' method for surface rock densities. *Pure and Applied Geophysics PAGEOPH* 110(1): 1927-1931. DOI: https://doi.org/10.1007/BF00876555.

REYNOLDS JM, 1997, *An Introduction to Applied and Environmental Geophysics*. Wiley. DOI: https://doi.org/10.1071/pvv2011n155other.

RITCHIE AS, PARASNIS DS and ADLER I, 1966, Methods in Geochemistry and Geophysics. *Methods in Geochemistry and Geophysics* 2(C). DOI: https://doi.org/10.1016/B978-1-4832-3031-3.50001-9.

RONG Y, BAI Y, REN M, LIANG M and WANG Z, 2023, Seismicity-based 3D model of ruptured seismogenic faults in the North–South Seismic Belt, China. *Frontiers in Earth Science* 10: 1023106. DOI: https://doi.org/10.3389/feart.2022.1023106.

ROSID MS and SIREGAR H, 2017, Determining fault structure using first horizontal derivative (FHD) and horizontal vertical diagonal maxima (HVDM) method: A comparative study. *AIP Conference Proceedings* 1862(1). DOI: https://doi.org/10.1063/1.4991275.

ROSID MS, 2023, Identification of geological structures in Sigi Regency, Central Sulawesi based on derivative analysis of gravity data. *International Journal of Geomate* 24(103): 26-33. DOI: https://doi.org/10.21660/2023.103.3426.

RUIYIN C, ZHU Y, ZHANG J, WEN A, HU S, LUO J and LI P, 2024, Determination of contributing area threshold and downscaling of topographic factors for small watersheds in hilly areas of purple soil. *Land* 13(8): 1193. DOI: https://doi.org/10.3390/land13081193.

SAIBI H, NISHIJIMA J, EHARA S and ABOUD E, 2006, Integrated gradient interpretation techniques for 2D and 3D gravity data interpretation. *Earth, Planets and Space* 58(7): 815-821. DOI: https://doi.org/10.1186/BF03351986.

SARKOWI M, 2010, Structure identification of Ulubelu geothermal area based on SVD data analysis of Bouguer anomaly (in Indonesian). *Jurnal Sains MIPA* 16(2).

SARKOWI M, MULYASARI R, DARMAWAN IGB and WIBOWO RC, 2022, Identification of the Semangko Fault in Sumatra, Indonesia, based on gradient gravity data analysis. *Songklanakarin Journal of Science and Technology* 44(6).

SCHWARTZ DP and COPPERSMITH KJ, 1984, Fault behavior and characteristic earthquakes: Examples from the Wasatch and San Andreas fault zones (USA). *Journal of Geophysical Research* 89(B7): 5681-5698. DOI: https://doi.org/10.1029/JB089iB07p05681.

SEMBIRING DK, INDRIANA RD and YULIANTO T, 2023, Subsurface model of Mt. Sinabung using the GGM-Plus satellite gravity data and Deconvolution Euler. *International Journal of Progressive Sciences and Technologies* 39(1). DOI: https://doi.org/10.52155/ijpsat.v39.1.5375.

STANLEY JM, 1977, Simplified gravity interpretation by gradients – The geological contact. *Geophysics* 42(6): 1230-1235. DOI: https://doi.org/10.1190/1.1440787.

SUKAMTO R, 1982, *Geological map of the Pangkajene and western part of Watampone Quadrangles, Sulawesi, scale 1:250,000*. Geological Research and Development Centre, Bandung, Indonesia.

SUMINTADIREJA P, DAHRIN D and GRANDIS H, 2018, A note on the use of the second vertical derivative (SVD) of gravity data with reference to Indonesian cases. *Journal of Engineering and Technological Sciences* 50(1): 127-139. DOI: https://doi.org/10.5614/j.eng.technol.sci.2018.50.1.9.

SUNIL PS, RADHAKRISHNA M, KURIAN PJ, MURTY BVS, SUBRAHMANYAM C, NAMBIAR CG, ARTS KP, ARUN SK and MOHAN SK, 2010, Crustal structure of the western part of the Southern Granulite Terrain of Indian Peninsular Shield derived from gravity data. *Journal of Asian Earth Sciences* 39(6): 551-564. DOI: https://doi.org/10.1016/j.jseaes.2010.04.028.

SUPENDI P, NUGRAHA AD, WIDIYANTORO S, ABDULLAH CI, PUSPITO NT, PALGUNADI KH, DARYONO D and WIYONO SH, 2019, Hypocenter relocation of the aftershocks of the Mw 7.5 Palu earthquake (September 28, 2018) and swarm earthquakes of Mamasa, Sulawesi, Indonesia, using the BMKG network data. *Geoscience Letters* 6(1). DOI: https://doi.org/10.1186/s40562-019-0148-9.

SUPENDI P, NUGRAHA AD, WIDIYANTORO S, PESICEK JD, THURBER CH, ABDULLAH CI, DARYONO D, WIYONO SH, SHIDDIQI HA and ROSALIA S, 2020, Relocated aftershocks and background seismicity in eastern Indonesia shed light on the 2018 Lombok and Palu earthquake sequences. *Geophysical Journal International* 221(3): 1845-1855.. DOI: https://doi.org/10.1093/gji/ggaa118.

SYAMSUDDIN E, MAULANA A, HAMZAH A and IRFAN UR, 2024, Assessing soil vulnerability in Petobo post-liquefaction zone, Palu, Central Sulawesi: A microzonation study utilizing microtremor measurements. *Journal of Degraded and Mining Lands Management* 11(3): 5805–5816. DOI: https://doi.org/10.15243/jdmlm.2024.113.5805.

TELFORD WM, GELDART LP and SHERIFF RE, 1990, *Applied Geophysics*. Cambridge University Press.

UMAR EP, 2023, Structural map of Sulawesi derived from gravity data and its implications for geothermal systems. *E3S Web of Conferences* 468: 04004. DOI: https://doi.org/10.1051/e3sconf/202346804004.

VALKANIOTIS S, GANAS A, TSIRONI V and BARBEROPOULOU A, 2018, A preliminary report on the M7.5 Palu earthquake co-seismic ruptures and landslides using image correlation techniques on optical satellite data. Zenodo. DOI: https://doi.org/10.5281/zenodo.1458130.

WALDHAUSER F and SCHAFF D P, 2007, Regional and teleseismic double-difference earthquake relocation using waveform cross-correlation and global bulletin data. *Journal of Geophysical Research: Solid Earth* 112(B12): 1-18. DOI: https://doi.org/10.1029/2007jb004938.

WALPERSDORF A, VIGNY C, SUBARYA C and MANURUNG P, 1998, Monitoring of the Palu-Koro fault (Sulawesi) by GPS. *Geophysical Research Letters* 25(13): 2313–2316. DOI: https://doi.org/10.1029/98GL01799.

WANG Y, FENG W, CHEN K and SAMSONOV S, 2019, Source characteristics of the 28 September 2018 Mw 7.4 Palu, Indonesia, earthquake derived from the Advanced Land Observation Satellite 2 data. *Remote Sensing* 11(17): 1999. DOI: https://doi.org/10.3390/rs11171999.

WATKINSON IM, 2011, Ductile flow in the metamorphic rocks of central Sulawesi. *Geological Society Special Publication* 355. DOI: https://doi.org/10.1144/SP355.8.

WELLS DL and COPPERSMITH KJ, 1994, New empirical relationships among magnitude, rupture length, rupture width, rupture area, and surface displacement. *Bulletin of the Seismological Society of America* 84(4): 974–1002. DOI: https://doi.org/10.1785/bssa0840040974.

WESSEL P, LUIS JF, UIEDA L, SCHARROO R, WOBBE F, SMITH WHF and TIAN D, 2019, The Generic Mapping Tools version 6. *Geochemistry, Geophysics, Geosystems* 20(11): 5556-5564. DOI: https://doi.org/10.1029/2019GC008515.

WILLIAMS JN, WEDMORE LNJ, SCHOLZ CA, KOLAWOLE F, WRIGHT LJM, SHILLINGTON DJ, FAGERENG Å, BIGGS J, MDALA H, DULANYA Z, MPHEPO F, CHINDANDALI PRN and WERNER

MJ, 2022, The Malawi active fault database: An onshore-offshore database for regional assessment of seismic hazard and tectonic evolution. *Geochemistry, Geophysics, Geosystems* 23(5): e2022GC010425. DOI: https://doi.org/10.1029/2022GC010425.

XU XW, YU GH, MA WT, KLINGER Y and TAPPONNIER P, 2008, Rupture behavior and deformation localization of the Kunlunshan earthquake (Mw7.8) and their tectonic implications. *Science in China, Series D: Earth Sciences* 51(10): 1361-1374. DOI: https://doi.org/10.1007/s11430-008-0099-z.

YU J and SUN D, 2022, A lower mantle slab below the East Asia margin constrained by seismic waveform complexity. *Journal of Geophysical Research: Solid Earth* 127(6): e2022JB024246. DOI: https://doi.org/10.1029/2022JB024246.

Received 25 March 2025
Accepted 12 June 2025